INTERNATIONAL JOURNAL OF HEALTH & MEDICAL RESEARCH
ISSN(print): 2833-213X, ISSN(online): 2833-2148
Volume 02 Issue 12 December 2023
DOI : 10.58806/ijhmr.2023.v2i12n06
Page No. 499-511

Molecular Docking Approach Reveals the Potential Role of *Psidium Guajava* Leaf Extract Compounds as Quorum-Sensing Inhibitors Targeting *Pseudomonas Aeruginosa*'s Lasr

Ayu Tri Agustin[1], Ahdiah Imroatul Muflihah[2], Anas Fadli Wijaya[3], Hartalina Mufidah[4], Jepri Riranto[5]
[1,2,3,4]Medical Laboratory Technology Study Program, Faculty of Health Sciences, Universitas dr. Soebandi, Indonesia, 68111
[5]Study Program of Nursing, Politeknik Yakpermas Banyumas, Indonesia, 53181
[1]0000-0001-6742-2249

ABSTRACT: Quorum-sensing LasR antagonism is evolving as a primary focus in promising new antivirulence approaches for treating bacterial infections. *Pseudomonas aeruginosa*'s LasR is a target receptor for developing alternative medicines in chronic wounds because it acts as an autoinducer in biofilm formation. Our research aims to predict the biofunction of Psidium guajava leaf water extract as an inhibitor of the quorum-sensing LasR of *Pseudomonas aeruginosa*. The 3D structures of five bioactive compounds (quercetin, gallocatechin, esculin, 3-sinapoylquinic acid, ellagic acid) and N-3-Oxo-Dodecanoyl-L-Homoserine Lactone (as positive control) were obtained from the PubChem Database. The Protein Data Bank database is used to download LasR. The active site of the LasR protein was determined using Molegro Virtual Docker 5.0. The docking simulation uses Molegro Virtual Docker 5.0 and Discovery Studio program version 21.1.1 for visualization. The results showed that the five compounds could bind to LasR at the active site and substrate binding, leading to the compound's potential as an antibacterial for *Pseudomonas aeruginosa* by inhibiting the quorum-sensing receptor LasR. The 3-sinapoylquinic acid-LasR complex shows the lowest binding energy, namely -311.2 kJ/mol.

KEYWORDS: anti-virulence, *autoinducer*, *in silico*, LasR, *P. aeruginosa*

INTRODUCTION

Prolonged hyperglycemia conditions cause a chronic metabolic disorder, anointed diabetes mellitus (DM). Diabetes mellitus is a significant health problem affecting most global populations (Burgess et al., 2021). The World Health Organization (WHO) reports that the prevalence of diabetes mellitus sufferers is estimated at nearly 500 million, and there is expected to be an increase. In 2019, the United States ranked third after China and India, with the highest cases of diabetes mellitus in 20-79-year-old adults (Ervita et al., 2022). Diabetic wound healing disorders have been experienced by around 25% of all diabetes mellitus patients and often result in lower limb amputation (Walicka et al., 2021). The resulting outcomes of lower extremity amputation have significant health costs, function and quality of life for patients (Gao et al., 2021; Walicka et al., 2021). The formation of bacterial biofilms in hyperglycemia conditions causes diabetes wounds to evolve increasingly chronic and demanding to treat (Burgess et al., 2021).

Pseudomonas aeruginosa is a gram-negative bacterium found as an agent of diabetic wound infection (Chin et al., 2023). These bacteria produce biofilms, a matrix that acts as a survival mechanism against the human immune system and antibiotic therapy. Forming a biofilm matrix in diabetic wounds triggers an inflammatory response, necrosis, decreased metabolic activity and cell division, and antibiotic treatment becomes resistant (Vestby et al., 2020). Ciprofloxacin antibiotics are generally used to treat infections and are known to be sensitive to *Pseudomonas aeruginosa* (Apridamayanti et al., 2016). However, extensive use of ciprofloxacin has the potential to be tolerant of Pseudomonas infection and severe side effects such as tendon damage and permanent nerve defects (Srivastava & Sivashanmugam, 2021; Rancan et al., 2019). Treatment strategies might have to target the causes of diabetic wound healing disorders and not induce adverse side effects (Burgess et al., 2021).

Herbal medicine has promising prospects for treating chronic wound infections. Various bioactive compounds from plants have the potential to be antimicrobial and anti-inflammatory agents, which allows the treatment of chronic infections (Abid et al., 2022; Tribudi et al., 2022). Ethnomedicinal studies report the biological function of guava leaf extract (Psidium guajava) to treat hypertension, obesity, diabetes, gastroenteritis, cancer, wounds and inflammation. Psidium guajava leaf extract is reported to have antibacterial activity and can enhance wound healing by inhibiting bacterial colonies, wound contraction and re-epithelialization (Purnamasari et al., 2022). Previous research showed that guava leaf methanol extract had a minimum inhibitory

concentration (MIC) of 256 µg/ml, which indicated efficacy in inhibiting *Bacillus subtilis*, *Escherichia coli*, *Staphylococcus flexneri*, and *Staphylococcus aureus* in vitro. Research of balms made from methanol extract of *Psidium guajava* leaves has been conducted in vivo on wounds induced by *S. aureus* infection in mice. The balm was applied topically to infected excision wounds and showed an increase in the rate of wound contraction (Ekom & Tamokou, 2018). Based on Liquid chromatography-mass spectrometry (LC/MS) analysis, *P. guajava* leaf extract shows the presence of phytochemicals such as quercetin, gallocatechin, esculin, 3-sinapoylquinic acid, and ellagic acid. Antibacterial activity was demonstrated by the highest inhibition zone of 4.1 ± 0.02 mm in *Bacillus subtilis* colonies (Sampath Kumar et al., 2021).

Computational studies have been carried out to reveal the mechanism of inhibition of zinc and chembridge compounds against the PqsA gene of *Pseudomonas aeruginosa*. The PqsA gene plays an essential role in signalling biofilm production through autoinducer induction (involved in communication between cells) (Shahab et al., 2023). Previous research showed that the compound (z)-5-octylidenethiazolidine-2,4-dione (TZD-C8) is an inhibitor of biofilm formation (Gholami et al., 2023). Previous research evaluated several compounds of betel leaf water extract (*Piper betle* L.), including eugenol, catechin, caffeic acid, quercetin, and ascorbic acid, showed antibacterial activity in *E. coli* through inhibiting the active site of FabB at residues ALA271, PRO272 and HIS298 (Agustin et al., 2022). So far, the cellular mechanism and potential role of bioactive compounds from water extracts of *P. guajava* leaves as inhibitors of the *Pseudomonas aeruginosa* LasR gene are unknown. Therefore, our study aims to predict the biofunction of *P. guajava* leaf aqueous extract to block the LasR gene. The LasR is a target protein in developing *P. aeruginosa* antibacterial drug candidates. LasR is a quorum-sensing-negative responsible for modulating *P. aeruginosa* virulence factors and biofilm formation (Heurlier et al., 2005; Liu et al., 2022). Inhibition of LasR by bioactive compounds may inhibit gene signalling cascades that lead to inhibition of biofilm formation.

METHODS DATA MINING

The compounds Quercetin (CID 5280343), Gallocatechin (CID 65084), Esculin (CID 5281417), 3-sinapoylquinic acid (CID 72193657), and Ellagic acid (CID 5281855) were downloaded from the PubChem Database (https://pubchem.ncbi.nlm. nih.gov/). The compound N-3-Oxo-Dodecanoyl-L-Homoserine Lactone was used as a comparison control by downloading it from the 2UV0 protein data bank database (Bottomley et al., 2007).

RETRIEVAL OF 3D PROTEIN STRUCTURES AND PREPARATION OF PROTEIN STRUCTURES

The Pseudomonas aeruginosa LasR target protein (PDB ID 2UV0) was downloaded from the Protein Data Bank database (Bottomley et al., 2007). The active site of the protein structure was predicted using the Molegro Virtual Docker 5.0 program with a maximum Molecular surface van der Waals parameter of 5. The active site of the *Pseudomonas aeruginosa* LasR protein on grid X= 39.71; Y = 32.58; Z = 35.56; Radius 23.

DOCKING SIMULATION

The target compounds and proteins were interacted with the Molegro virtual docker program with a specific grid, namely the active site grid (X= 39.71; Y= 32.58; Z= 35.56; Radius 23) (Bitencourt-Ferreira & de Azevedo, 2019). Docking parameters with Molegro virtual docker are Score Function Moldock Score [Grid]; grid resolution 0.30; algorithm MolDock SE; Number of Runs 10, Max iterations 1500; max population size 50; pose generation energy threshold 100, tries 10 – 30; simplex evolution max steps 300; neighbour distance factor 1.00; multiple poses number of poses 5; energy threshold 0.00; cluster similar poses RMSD threshold 1.

DATA ANALYSIS

The docking results with Molegro virtual docking version 5 were combined with proteins (superimposed) using PyMol version 2.2 software. The Discovery Studio program version 21.1.1 was used for docking visualization to display 3D and 2D views and interactions (Agustin et al., 2020).

RESULTS AND DISCUSSION

The molecular docking results between the bioactive compounds of *P. guajava* leaf water extract and LasR were indicated by molecular interactions, types of chemical bonds, and binding energy (Table 1). LasR consists of two domains: the C-terminal and the N-terminal domains, which act as multimerization regulators. Amino acid residues 88 to 160 in the N-terminal domain can inhibit multimerization in the C-terminal domain (Kiratisin et al., 2002). The complex 3D structure of the interaction between the compound and LasR shows binding on different sides. Gallocatechin and Quercetin compounds bind to the LasR inhibitor site, while Esculin, Ellagic acid, and 3-sinapoylquinic acid bind to the LasR substrate (Figure 1a).

Molecular Docking Approach Reveals the Potential Role of *Psidium Guajava* Leaf Extract Compounds as Quorum-Sensing Inhibitors Targeting *Pseudomonas Aeruginosa*'s Lasr

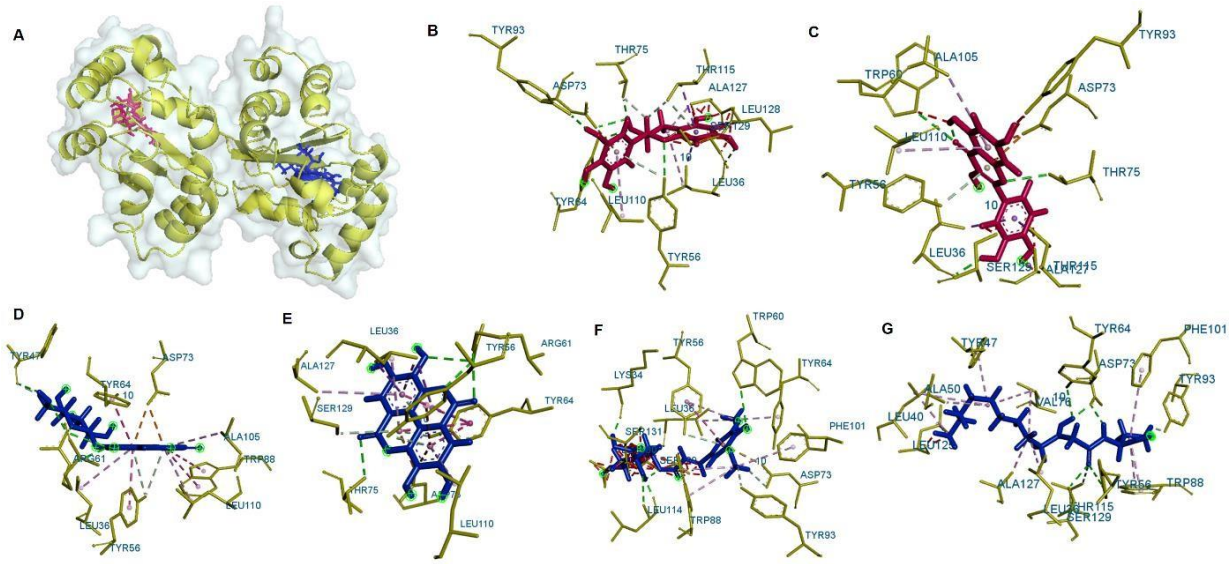

Figure 1. 3D appearance of the complex compound - LASR protein, A. superimposed compound

- LASR protein, B. Gallocatechin, C. Quercetin, D. Esculin, E. Ellagic acid, F. 3- sinapoylquinic acid, G. N-3-Oxo -Dodecanoyl-L-Homoserine Lactone, LASR protein is illustrated in yellow cartoon, Gallocatechin and Quercetin compounds are shown in pink, while the other four compounds are shown in blue.

The interaction between gallocatechin and LasR complex involves the amino acid residues TYR56, TYR64, ASP73, THR75, LEU36, TYR93, THR75, as well as THR115, ALA127,

LEU128, and SER129. Hydrogen bonds, hydrophobic bonds, and van der Waals forces stabilize the gallocatechin-LasR complex (as shown in Figure 1b). Quercetin binds to 8 amino acid residues, including TRP60, THR75, LEU36, ASP73, TYR56, THR115, ALA105, and LEU110, with

hydrogen bonds, van der Waals forces, and hydrophobic interactions stabilizing this interaction (as shown in Figure 1c). On the other hand, esculin binds to 9 amino acid residues, including ARG61, TYR47, ASP73, TYR56, TYR64, TRP88, LEU36, ALA105, and LEU110 of LasR, and

the complex is maintained by van der Waals forces, hydrogen bonds, and hydrophobic interactions (as shown in Figure 1d). Ellagic acid binds to LasR at ARG61, THR75, ASP73, TYR56, TYR64, SER129, LEU36, ALA127, and LEU110 residues. Hydrogen bonding, hydrophobicity, and van der Waals forces are responsible for strengthening the ellagic acid-LasR complex (as shown in Figure 1e). Lastly, the amino acid residues TRP60, LEU114, LEU36, LYS34, ASP73, TYR93, TYR56, TYR64, TRP88, PHE101, SER129, LEU130, and SER131 from LasR are successfully bound by 3-sinapoylquinic acid through hydrogen bonds, van der Waals forces, and hydrophobic interactions (as shown in Fig. 1f). Figure 1g shows the compound N-3-Oxo-Dodecanoyl-L-Homoserine Lactone used as a control and a LasR protein substrate. Based on the 3D structure and bound amino acid residues, two types of inhibition, namely Gallocatechin and Quercetin compounds, have the potential to act as LasR inhibitors. The other three compounds, esculin, ellagic acid, and 3-sinapoylquinic acid, inhibit LasR in the substrate region and are predicted to be competitive inhibitors. *Pseudomonas aeruginosa*'s quorum-sensing response is regulated by LasR, which is a primary quorum-sensing signalling receptor that controls the transcription of virulence factors for optimal expression. This response is modulated by integrating cell communication with environmental and metabolic cues (Longo et al., 2013). The binding of residues to LasR's active site can affect the cascade of autoinducer genes, leading to alterations in the quorum-sensing response of *Pseudomonas aeruginosa* (McCready et al., 2019).

The energy binding values of the LasR compound–protein complex range from -311.2 kJ/mol to -295.667 kJ/mol. The bond energy values of 3-sinapoylquinic acid, Esculin, Ellagic acid, Gallocatechin, Quercetin, and N-3-Oxo-Dodecanoyl-L-Homoserine Lactone are compared in Table 1. The variation in bond energy in each LasR compound-protein complex is influenced by variations in the type of bond and the number of hydrogen and hydrophobic bonds. The bonds formed between the compound and the LasR protein include hydrophobic interactions, hydrogen bonds, van der Waals forces, and unfavourable bonds (as shown in Figure 2). If the bond energy value is low, then it indicates a potent interaction between the compound and protein. The strength of the interaction between the ligand and target protein is directly proportional to the decrease in binding energy. The compound with the highest ability to bind LasR is 3-sinapoylquinic acid, with a binding energy of -311.2 kJ/mol.

Molecular Docking Approach Reveals the Potential Role of *Psidium Guajava* Leaf Extract Compounds as Quorum-Sensing Inhibitors Targeting *Pseudomonas Aeruginosa*'s Lasr

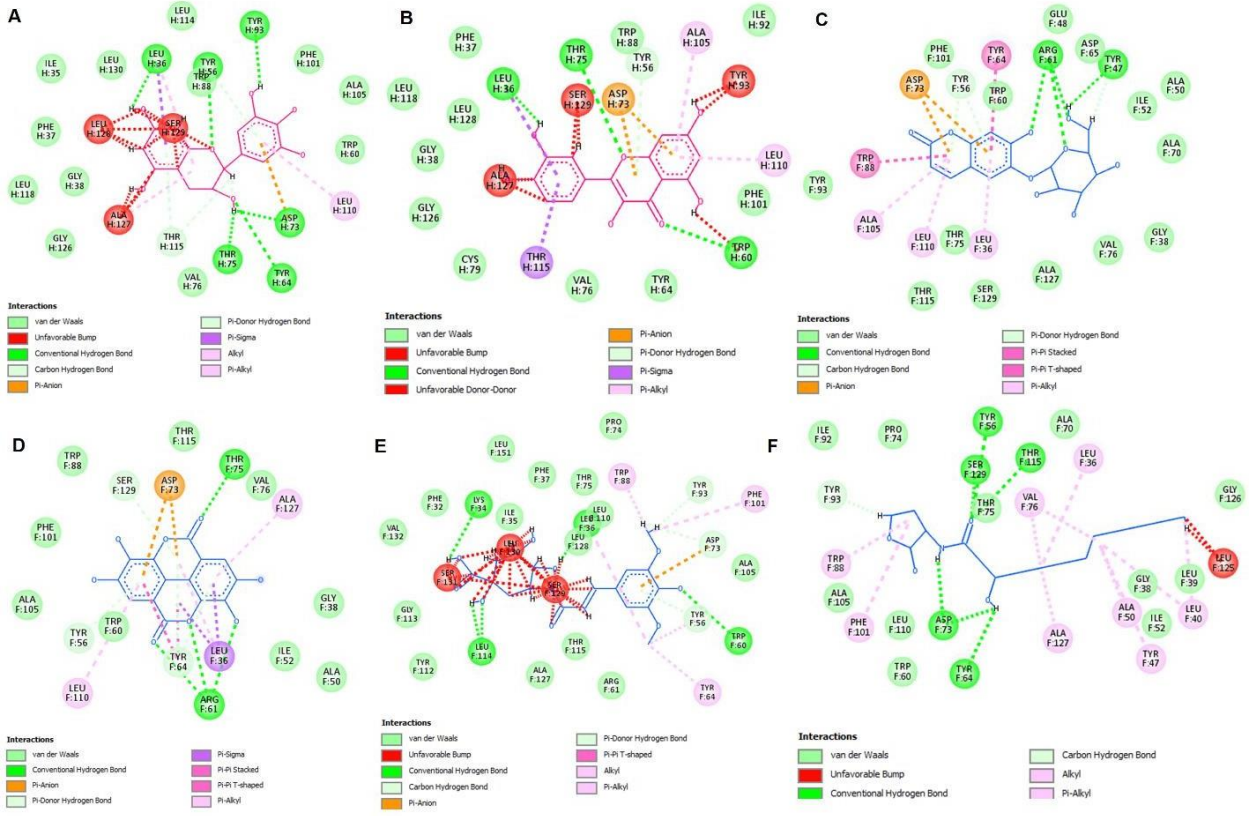

Figure 2. The 2D structure of the compound–LASR complex, A. Gallocatechin, B. Quercetin, C. Esculin, D. Ellagic acid, E. 3-sinapoylquinic acid, F. N-3-Oxo-Dodecanoyl-L-Homoserine Lactone

Table 1. Interactions between five compounds of *Psidium guajava* leaf water extracts and LASR

Ligands	Binding Energy (kJ/mol)	Interaction	Distance (A)	Category	Types
Gallocatechin	-306,4	H:TYR56:OH - :10:O1	2,9311	Hydrogen Bond	Conventional Hydrogen Bond
		H:TYR64:OH - :10:O2	3,18478	Hydrogen Bond	Conventional Hydrogen Bond
		:10:H8 - H:ASP73:OD2	2,44027	Hydrogen Bond	Conventional Hydrogen Bond
		:10:H8 - H:THR75:OG1	2,04649	Hydrogen Bond	Conventional Hydrogen Bond
		:10:H11 - H:LEU36:O	2,29006	Hydrogen Bond	Conventional Hydrogen Bond
		:10:H12 - H:TYR93:OH	2,28888	Hydrogen Bond	Conventional Hydrogen Bond
		:10:H2 - H:THR75:OG1	2,39174	Hydrogen Bond	Carbon Hydrogen Bond
		:10:H2 - H:THR115:OG1	2,47528	Hydrogen Bond	Carbon Hydrogen Bond
		H:ASP73:OD2 - :10	3,60127	Electrostatic	Pi-Anion

Ligands	Binding Energy (kJ/mol)	Interaction	Distance (A)	Category	Types
		H:TYR56:OH - :10	3,9352	Hydrogen Bond	Pi-Donor Hydrogen Bond
		H:THR115:OG1 - :10	3,92448	Hydrogen Bond	Pi-Donor Hydrogen Bond
		H:LEU36:CD2 - :10	3,9428	Hydrophobic	Pi-Sigma

H:THR115:CG2 - :10	3,63514	Hydrophobic	Pi-Sigma
H:LEU36 - :10	4,68235	Hydrophobic	Alkyl
H:ALA127 - :10	3,88945	Hydrophobic	Alkyl
:10 - H:LEU110	5,29778	Hydrophobic	Pi-Alkyl
H:ALA127:CA - :10:O3	1,96691	Unfavorable	Unfavorable Bump
H:ALA127:CA - :10:H10	1,44171	Unfavorable	Unfavorable Bump
H:ALA127:C - :10:O3	2,03469	Unfavorable	Unfavorable Bump
H:ALA127:C - :10:H10	1,11497	Unfavorable	Unfavorable Bump
H:ALA127:CB - :10:O3	1,27761	Unfavorable	Unfavorable Bump
H:ALA127:CB - :10:C7	2,3397	Unfavorable	Unfavorable Bump
H:ALA127:CB - :10:H10	1,66116	Unfavorable	Unfavorable Bump
H:LEU128:N - :10:H9	1,46322	Unfavorable	Unfavorable Bump
H:LEU128:CA - :10:C11	2,15821	Unfavorable	Unfavorable Bump
H:LEU128:CA - :10:H9	1,24534	Unfavorable	Unfavorable Bump
H:LEU128:C - :10:O4	1,41772	Unfavorable	Unfavorable Bump
H:LEU128:C - :10:C11	1,8897	Unfavorable	Unfavorable Bump
H:LEU128:C - :10:C12	1,68603	Unfavorable	Unfavorable Bump
H:LEU128:C - :10:H9	1,77324	Unfavorable	Unfavorable Bump
H:SER129:N - :10:O4	0,791988	Unfavorable	Unfavorable Bump
H:SER129:N - :10:C8	1,88234	Unfavorable	Unfavorable Bump
H:SER129:N - :10:C11	1,65281	Unfavorable	Unfavorable Bump
H:SER129:N - :10:C12	0,612079	Unfavorable	Unfavorable Bump
H:SER129:N - :10:H11	1,36959	Unfavorable	Unfavorable Bump
H:SER129:CA - :10:O4	1,53972	Unfavorable	Unfavorable Bump

Ligands	Binding Energy (kJ/mol)	Interaction	Distance (A)	Category	Types
		H:SER129:CA - :10:C8	1,22455	Unfavorable	Unfavorable Bump
		H:SER129:CA - :10:C12	1,37261	Unfavorable	Unfavorable Bump
		H:SER129:CA - :10:H5	1,13979	Unfavorable	Unfavorable Bump
		H:SER129:C - :10:O4	2,03274	Unfavorable	Unfavorable Bump
		H:SER129:CB - :10:O1	1,97855	Unfavorable	Unfavorable Bump

		H:SER129:CB - :10:C6	1,43419	Unfavorable	Unfavorable Bump
		H:SER129:CB - :10:C8	0,682183	Unfavorable	Unfavorable Bump
		H:SER129:CB - :10:C12	2,02473	Unfavorable	Unfavorable Bump
		H:SER129:CB - :10:H5	0,780732	Unfavorable	Unfavorable Bump
		H:SER129:OG - :10:O1	1,41864	Unfavorable	Unfavorable Bump
		H:SER129:OG - :10:C4	1,70267	Unfavorable	Unfavorable Bump
		H:SER129:OG - :10:C6	0,558903	Unfavorable	Unfavorable Bump
		H:SER129:OG - :10:C8	1,34574	Unfavorable	Unfavorable Bump
		H:SER129:HN - :10:O4	1,543	Unfavorable	Unfavorable Bump
		H:SER129:HN - :10:C12	1,17807	Unfavorable	Unfavorable Bump
		H:SER129:HN - :10:H11	1,37911	Unfavorable	Unfavorable Bump
Quercetin	-305,2	H:TRP60:NE1 - :10:O4	3,12461	Hydrogen Bond	Conventional Hydrogen Bond
		H:THR75:OG1 - :10:O1	2,82235	Hydrogen Bond	Conventional Hydrogen Bond
		:10:H7 - :10:O4	1,79284	Hydrogen Bond	Conventional Hydrogen Bond
		:10:H9 - H:LEU36:O	2,12321	Hydrogen Bond	Conventional Hydrogen Bond
		H:ASP73:OD2 - :10	3,20955	Electrostatic	Pi-Anion
		H:ASP73:OD2 - :10	3,86955	Electrostatic	Pi-Anion
		H:TYR56:OH - :10	3,73857	Hydrogen Bond	Pi-Donor Hydrogen Bond
		H:LEU36:CD2 - :10	3,85522	Hydrophobic	Pi-Sigma
		H:THR115:CG2 - :10	3,57308	Hydrophobic	Pi-Sigma
		:10 - H:ALA105	4,97759	Hydrophobic	Pi-Alkyl
		:10 - H:LEU110	5,30364	Hydrophobic	Pi-Alkyl

Ligands	Binding Energy (kJ/mol)	Interaction	Distance (A)	Category	Types
Esculin	-309,8	F:ARG61:NE - :10:O8	3,01859	Hydrogen Bond	Conventional Hydrogen Bond
		F:ARG61:NH2 - :10:O1	3,26088	Hydrogen Bond	Conventional Hydrogen Bond
		F:ARG61:NH2 - :10:O6	3,15499	Hydrogen Bond	Conventional Hydrogen Bond
		F:ARG61:NH2 - :10:O8	3,06864	Hydrogen Bond	Conventional Hydrogen Bond
		:10:H11 - F:TYR47:O	2,33377	Hydrogen Bond	Conventional Hydrogen Bond
		:10:H6 - F:TYR47:O	1,93103	Hydrogen Bond	Carbon Hydrogen Bond
		F:ASP73:OD2 - :10	3,99646	Electrostatic	Pi-Anion
		F:ASP73:OD2 - :10	3,67863	Electrostatic	Pi-Anion
		F:TYR56:OH - :10	4,13494	Hydrogen Bond	Pi-Donor Hydrogen Bond
		F:TYR56:OH - :10	4,00884	Hydrogen Bond	Pi-Donor Hydrogen Bond
		F:TYR64 - :10	4,08724	Hydrophobic	Pi-Pi Stacked
		F:TRP88 - :10	5,74968	Hydrophobic	Pi-Pi Stacked
		F:TRP88 - :10	4,81199	Hydrophobic	Pi-Pi Stacked
		F:TYR56 - :10	4,41517	Hydrophobic	Pi-Pi T-shaped
		:10 - F:LEU36	5,0831	Hydrophobic	Pi-Alkyl
		:10 - F:ALA105	5,22616	Hydrophobic	Pi-Alkyl
		:10 - F:LEU110	4,95625	Hydrophobic	Pi-Alkyl
Ellagic acid	-306,4	F:ARG61:NE - :10:O7	3,00652	Hydrogen Bond	Conventional Hydrogen Bond
		F:ARG61:NH2 - :10:O1	2,59682	Hydrogen Bond	Conventional Hydrogen Bond
		F:ARG61:NH2 - :10:O3	3,0021	Hydrogen Bond	Conventional Hydrogen Bond
		F:THR75:OG1 - :10:O8	2,6285	Hydrogen Bond	Conventional Hydrogen Bond
		F:ASP73:OD2 - :10	3,28461	Electrostatic	Pi-Anion
		F:ASP73:OD2 - :10	3,75509	Electrostatic	Pi-Anion
		F:TYR56:OH - :10	3,99049	Hydrogen Bond	Pi-Donor Hydrogen Bond
		F:TYR64:OH - :10	3,772	Hydrogen Bond	Pi-Donor Hydrogen Bond
		F:TYR64:OH - :10	3,614	Hydrogen Bond	Pi-Donor Hydrogen Bond
		F:SER129:OG - :10	4,11509	Hydrogen Bond	Pi-Donor Hydrogen Bond
		F:LEU36:CD1 - :10	3,80335	Hydrophobic	Pi-Sigma

Ligands	Binding Energy (kJ/mol)	Interaction	Distance (A)	Category	Types
		F:LEU36:CD1 - :10	3,5081	Hydrophobic	Pi-Sigma
		F:LEU36:CD2 - :10	3,33275	Hydrophobic	Pi-Sigma
		F:TYR64 - :10	4,71531	Hydrophobic	Pi-Pi Stacked

		F:TYR64 - :10	3,50521	Hydrophobic	Pi-Pi Stacked
		F:TYR64 - :10	4,86392	Hydrophobic	Pi-Pi Stacked
		F:TYR64 - :10	4,43592	Hydrophobic	Pi-Pi Stacked
		F:TYR56 - :10	4,55868	Hydrophobic	Pi-Pi T-shaped
		:10 - F:LEU36	4,83797	Hydrophobic	Pi-Alkyl
		:10 - F:ALA127	5,30552	Hydrophobic	Pi-Alkyl
		:10 - F:LEU110	5,49531	Hydrophobic	Pi-Alkyl
3-sinapoylquinic acid	-311,2	F:TRP60:NE1 - :10:O10	3,15336	Hydrogen Bond	Conventional Hydrogen Bond
		F:LEU114:N - :10:O2	3,18264	Hydrogen Bond	Conventional Hydrogen Bond
		:10:H8 F:LEU114:O	-1,67934	Hydrogen Bond	Conventional Hydrogen Bond
		:10:H8 - :10:O1	2,18234	Hydrogen Bond	Conventional Hydrogen Bond
		:10:H9 - F:LEU36:O	1,87206	Hydrogen Bond	Conventional Hydrogen Bond
		:10:H11 - F:LYS34:O	1,87316	Hydrogen Bond	Conventional Hydrogen Bond
		:10:H1 - F:LEU36:O	2,84639	Hydrogen Bond	Carbon Hydrogen Bond
		:10:H18 - F:ASP73:OD1	2,64817	Hydrogen Bond	Carbon Hydrogen Bond
		:10:H19 - F:TYR93:OH	2,36386	Hydrogen Bond	Carbon Hydrogen Bond
		F:ASP73:OD2 - :10	3,66302	Electrostatic	Pi-Anion
		F:TYR56:OH - :10	3,33947	Hydrogen Bond	Pi-Donor Hydrogen Bond
		F:TYR56 - :10	4,73589	Hydrophobic	Pi-Pi T-shaped
		:10:C18 - F:LEU36	3,78588	Hydrophobic	Alkyl
		F:TYR56 - :10:C18	4,83108	Hydrophobic	Pi-Alkyl
		F:TYR64 - :10:C18	3,78818	Hydrophobic	Pi-Alkyl
		F:TRP88 - :10:C17	4,45562	Hydrophobic	Pi-Alkyl
		F:TRP88 - :10:C17	4,33733	Hydrophobic	Pi-Alkyl
		F:PHE101 - :10:C17	4,81522	Hydrophobic	Pi-Alkyl
		F:SER129:N - :10:O1	1,99202	Unfavorable	Unfavorable Bump

Ligands	**Binding Energy (kJ/mol)**	**Interaction**	**Distance (A)**	**Category**	**Types**
		F:SER129:N - :10:O3	1,85112	Unfavorable	Unfavorable Bump
		F:SER129:N - :10:O7	1,71595	Unfavorable	Unfavorable Bump
		F:SER129:N - :10:C8	1,87888	Unfavorable	Unfavorable Bump
		F:SER129:N - :10:H9	1,69218	Unfavorable	Unfavorable Bump
		F:SER129:CA - :10:O1	0,545034	Unfavorable	Unfavorable Bump
		F:SER129:CA - :10:C2	1,62316	Unfavorable	Unfavorable Bump

		F:SER129:CA - :10:O7	1,91653	Unfavorable	Unfavorable Bump
		F:SER129:CA - :10:C8	1,18926	Unfavorable	Unfavorable Bump
		F:SER129:C - :10:C1	2,3164	Unfavorable	Unfavorable Bump
		F:SER129:C - :10:O1	1,32207	Unfavorable	Unfavorable Bump
		F:SER129:C - :10:C2	0,760102	Unfavorable	Unfavorable Bump
		F:SER129:C - :10:C3	1,79381	Unfavorable	Unfavorable Bump
		F:SER129:C - :10:O3	2,16438	Unfavorable	Unfavorable Bump
		F:SER129:C - :10:C5	1,23872	Unfavorable	Unfavorable Bump
		F:SER129:C - :10:C6	1,89363	Unfavorable	Unfavorable Bump
		F:SER129:C - :10:H1	1,80451	Unfavorable	Unfavorable Bump
		F:SER129:O - :10:C2	1,08183	Unfavorable	Unfavorable Bump
		F:SER129:O - :10:C3	2,03535	Unfavorable	Unfavorable Bump
		F:SER129:O - :10:O3	1,9404	Unfavorable	Unfavorable Bump
		F:SER129:O - :10:C5	0,81752	Unfavorable	Unfavorable Bump
		F:SER129:O - :10:C6	2,17049	Unfavorable	Unfavorable Bump
		F:SER129:O - :10:H1	1,47215	Unfavorable	Unfavorable Bump
		F:SER129:O - :10:H6	1,09463	Unfavorable	Unfavorable Bump
		F:SER129:CB - :10:O1	1,43769	Unfavorable	Unfavorable Bump
		F:SER129:CB - :10:C2	2,15588	Unfavorable	Unfavorable Bump
		F:SER129:CB - :10:O7	1,95503	Unfavorable	Unfavorable Bump

Ligands	**Binding Energy (kJ/mol)**	**Interaction**	**Distance (A)**	**Category**	**Types**
		F:SER129:CB - :10:C8	0,783713	Unfavorable	Unfavorable Bump
		F:SER129:CB - :10:C9	0,882368	Unfavorable	Unfavorable Bump
		F:SER129:CB - :10:C10	2,08968	Unfavorable	Unfavorable Bump
		F:SER129:CB - :10:H12	1,4505	Unfavorable	Unfavorable Bump
		F:SER129:OG - :10:O7	1,66998	Unfavorable	Unfavorable Bump
		F:SER129:OG - :10:C8	1,33255	Unfavorable	Unfavorable Bump
		F:SER129:OG - :10:C9	1,32715	Unfavorable	Unfavorable Bump
		F:SER129:OG - :10:C10	1,4009	Unfavorable	Unfavorable Bump

F:SER129:OG - :10:H13	1,31807	Unfavorable	Unfavorable Bump
F:LEU130:N - :10:C1	1,38412	Unfavorable	Unfavorable Bump
F:LEU130:N - :10:O1	2,04578	Unfavorable	Unfavorable Bump
F:LEU130:N - :10:C2	1,90505	Unfavorable	Unfavorable Bump
F:LEU130:N - :10:O2	1,57859	Unfavorable	Unfavorable Bump
F:LEU130:N - :10:C3	1,88645	Unfavorable	Unfavorable Bump
F:LEU130:N - :10:C4	1,60745	Unfavorable	Unfavorable Bump
F:LEU130:N - :10:C5	2,08333	Unfavorable	Unfavorable Bump
F:LEU130:N - :10:C6	1,62408	Unfavorable	Unfavorable Bump
F:LEU130:N - :10:H7	1,66655	Unfavorable	Unfavorable Bump
F:LEU130:N - :10:H8	1,2787	Unfavorable	Unfavorable Bump
F:LEU130:CA - :10:C1	1,0708	Unfavorable	Unfavorable Bump
F:LEU130:CA - :10:O2	2,06396	Unfavorable	Unfavorable Bump
F:LEU130:CA - :10:C3	2,22173	Unfavorable	Unfavorable Bump
F:LEU130:CA - :10:C4	0,473208	Unfavorable	Unfavorable Bump
F:LEU130:CA - :10:C6	1,83678	Unfavorable	Unfavorable Bump
F:LEU130:CA - :10:C7	2,06559	Unfavorable	Unfavorable Bump
F:LEU130:CA - :10:H4	1,31604	Unfavorable	Unfavorable Bump

Ligands	Binding Energy (kJ/mol)	Interaction	Distance (A)	Category	Types
		F:LEU130:CA - :10:H5	1,28361	Unfavorable	Unfavorable Bump
		F:LEU130:C - :10:C1	1,24876	Unfavorable	Unfavorable Bump
		F:LEU130:C - :10:O2	1,85299	Unfavorable	Unfavorable Bump
		F:LEU130:C - :10:C4	1,92254	Unfavorable	Unfavorable Bump
		F:LEU130:C - :10:O5	1,45717	Unfavorable	Unfavorable Bump
		F:LEU130:C - :10:O6	1,94675	Unfavorable	Unfavorable Bump
		F:LEU130:C - :10:C7	0,899125	Unfavorable	Unfavorable Bump
		F:LEU130:O - :10:C1	2,04799	Unfavorable	Unfavorable Bump
		F:LEU130:O - :10:O2	1,6576	Unfavorable	Unfavorable Bump
		F:LEU130:O - :10:C7	1,82842	Unfavorable	Unfavorable Bump
		F:LEU130:CB - :10:C4	1,1691	Unfavorable	Unfavorable Bump
		F:LEU130:CB - :10:O4	2,14917	Unfavorable	Unfavorable Bump
		F:LEU130:CB - :10:C6	1,86872	Unfavorable	Unfavorable Bump
		F:LEU130:CB - :10:H4	1,67172	Unfavorable	Unfavorable Bump
		F:LEU130:CB - :10:H5	0,584008	Unfavorable	Unfavorable Bump
		F:LEU130:CB - :10:H10	1,8283	Unfavorable	Unfavorable Bump
		F:LEU130:CG - :10:C4	2,1357	Unfavorable	Unfavorable Bump
		F:LEU130:CG - :10:O4	0,788043	Unfavorable	Unfavorable Bump
		F:LEU130:CG - :10:C6	1,62356	Unfavorable	Unfavorable Bump
		F:LEU130:CG - :10:H10	0,462482	Unfavorable	Unfavorable Bump
		F:LEU130:CD1 - :10:O4	1,74475	Unfavorable	Unfavorable Bump
		F:LEU130:CD1 - :10:H10	1,14062	Unfavorable	Unfavorable Bump
		F:LEU130:CD2 - :10:O4	1,83313	Unfavorable	Unfavorable Bump
		F:LEU130:CD2 - :10:H10	1,54811	Unfavorable	Unfavorable Bump
		F:SER131:N - :10:C1	2,09011	Unfavorable	Unfavorable Bump
		F:SER131:N - :10:O5	0,890109	Unfavorable	Unfavorable Bump

CONCLUSION

All five compounds of *Psidium guajava* leaf water extracts have the potential to act as antibacterials against *P. aeruginosa* by two mechanisms. Gallocatechin and Quercetin compounds inhibit LasR on the inhibitor side. Esculin, Ellagic acid, and 3-sinapoylquinic acid inhibit LasR competitively on the substrate binding.

ACKNOWLEDGEMENT

This research was funded by the PDP Research Grant of LPPM Universitas dr. Soebandi Jember.

REFERENCES

1) Abid HMU, Hanif M, Mahmood K, Aziz M, Abbas G, Latif H (2022) Wound-Healing and Antibacterial Activity of the Quercetin–4-Formyl Phenyl Boronic Acid Complex against Bacterial Pathogens of Diabetic Foot Ulcer. *ACS Omega* 7: 24415–24422. https://doi.org/10.1021/acsomega.2c01819
2) Agustin AT, Safitri A, Fatchiyah F (2020) An in Silico Approach Reveals the Potential Function of Cyanidin-3-o-glucoside of Red Rice in Inhibiting the Advanced Glycation End Products (AGES)-Receptor (RAGE) Signaling Pathway. *Acta Inform. Medica* 28: 170–179. https://doi.org/10.5455/aim.2020.28.170-179
3) Agustin AT, Julianto E, Julianus J, Riranto J (2022) Potential Role of Betel Leaf (Piper betle L.) Water Extract as Antibacterial Escherichia coli Through Inhibition of β-Ketoacyl-[Acyl Carrier Protein] Synthase I. *Trop. J. Nat. Prod. Res.* 6: 1802–1808. https://doi.org/10.26538/tjnpr/v6i11.10
4) Apridamayanti P, Meilinasary KA, Sari R (2016) Antibiotic Sensitivity in Pseudomonas aeruginosa of Diabetic Patient's Foot Ulcer. *Pharm. Sci. Res.* 3: 80–87. https://doi.org/10.7454/psr.v3i2.3289
5) Bitencourt-Ferreira G, de Azevedo WFJ (2019) Molegro Virtual Docker for Docking. *Methods Mol. Biol.* 2053: 149–167. https://doi.org/10.1007/978-1-4939-9752-7_10
6) Bottomley MJ, Muraglia E, Bazzo R, Carfi A (2007) Molecular insights into quorum sensing in the human pathogen Pseudomonas aeruginosa from the structure of the virulence regulator LasR bound to its autoinducer. *J. Biol. Chem.* 282: 13592–13600. https://doi.org/10.1074/jbc.M700556200
7) Burgess JL, Wyant WA, Abdo Abujamra B, Kirsner RS, Jozic I (2021) Diabetic Wound-Healing Science. *Medicina (B. Aires).* 57: 1072. https://doi.org/10.3390/medicina57101072
8) Chin JD, Zhao L, Mayberry TG, Cowan BC, Wakefield MR, Fang Y (2023) Photodynamic Therapy, Probiotics, Acetic Acid, and Essential Oil in the Treatment of Chronic Wounds Infected with Pseudomonas aeruginosa. *Pharmaceutics* 15: 1721. https://doi.org/10.3390/pharmaceutics15061721
9) Ekom SE, Tamokou JDD (2018) Methanol Leaves Extract of Psidium guajava Linn. Exhibited Antibacterial and Wound Healing Activities. *Int. J. Curr. Microbiol. Appl. Sci.* 7: 4008–4023. https://doi.org/10.20546/ijcmas.2018.707.467
10) Ervita L, Hastuti L, Wuriani W (2022) Study Phenomenology Of Wound Care In Diabetic Foot Ulcer (DFU) Patients With Theory Of Planned Behavior Approach. *Int. J. Progress. Sci. Technol.* 34: 517. https://doi.org/10.52155/ijpsat.v34.2.4628
11) Gao D, Zhang Y, Bowers DT, Liu W, Ma M (2021) Functional hydrogels for diabetic wound management. *APL Bioeng.* 5: 31503. https://doi.org/10.1063/5.0046682
12) Gholami A, Minai-Tehrani D, Farewell A, Eriksson LA (2023) Discovery of novel inhibitors for Pseudomonas aeruginosa lipase enzyme from in silico and in vitro studies. *J. Biomol. Struct. Dyn.* 0: 1–14. https://doi.org/10.1080/07391102.2023.2203258
13) Heurlier K, Dénervaud V, Haenni M, Guy L, Krishnapillai V, Haas D (2005) Quorum-sensing- negative (lasR) mutants of Pseudomonas aeruginosa avoid cell lysis and death. *J. Bacteriol.* 187: 4875–83. https://doi.org/10.1128/JB.187.14.4875-4883.2005
14) Kiratisin P, Tucker KD, Passador L (2002) LasR, a Transcriptional Activator of Pseudomonas aeruginosa Virulence Genes, Functions as a Multimer. *J. Bacteriol.* 184: 4912–4919. https://doi.org/10.1128/JB.184.17.4912-4919.2002
15) Liu Y, Ahator S Dela, Wang H, Feng Q, Xu Y, Li C, Zhou X, Zhang L-H (2022) Microevolution of the mexT and lasR Reinforces the Bias of Quorum Sensing System in Laboratory Strains of Pseudomonas aeruginosa PAO1. *Front. Microbiol.* 13: 1–15. https://doi.org/10.3389/fmicb.2022.821895
16) Longo F, Rampioni G, Bondì R, Imperi F, Fimia GM, Visca P, Zennaro E, Leoni L (2013) A New
17) Transcriptional Repressor of the Pseudomonas aeruginosa Quorum Sensing Receptor Gene lasR. *PLoS One* 8: 1–9. https://doi.org/10.1371/journal.pone.0069554
18) McCready AR, Paczkowski JE, Henke BR, Bassler BL (2019) Structural determinants driving homoserine lactone ligand selection in the Pseudomonas aeruginosa LasR quorum-sensing receptor. *Proc. Natl. Acad. Sci. U. S. A.* 116: 245–254. https://doi.org/10.1073/pnas.1817239116
19) Purnamasari L, Victoria Carolino M, F. dela Cruz J (2022) The Antibacterial Properties of Psidium guajava Leaf Extract as a Wound Healing Agent of Laboratory Animals: a Review. *Biotropika J. Trop. Biol.*10:154–160. https://doi.org/10.21776/ub.biotropika.2022.010.02.10
20) Rancan, Contardi, Jurisch, Blume-Peytavi, Vogt, Bayer, Schaudinn (2019) Evaluation of Drug Delivery and Efficacy of Ciprofloxacin-Loaded Povidone Foils and Nanofiber Mats in a Wound-Infection Model Based on Ex Vivo Human Skin. *Pharmaceutics* 11: 527. https://doi.org/10.3390/pharmaceutics11100527

21) Sampath Kumar NS, Sarbon NM, Rana SS, Chintagunta AD, Prathibha S, Ingilala SK, Jeevan Kumar SP, Sai Anvesh B, Dirisala VR (2021) Extraction of bioactive compounds from Psidium guajava leaves and its utilization in preparation of jellies. *AMB Express* 11: 36. https://doi.org/10.1186/s13568-021-01194-9
22) Shahab M, Danial M, Khan T, Liang C, Duan X, Wang D, Gao H, Zheng G (2023) In Silico Identification of Lead Compounds for Pseudomonas Aeruginosa PqsA Enzyme: Computational Study to Block Biofilm Formation. *Biomedicines* 11: 961. https://doi.org/10.3390/biomedicines11030961
23) Srivastava P, Sivashanmugam K (2021) Efficacy of sub-MIC level of meropenem and ciprofloxacin against extensive drug-resistant (XDR) Pseudomonas aeruginosa isolates of diabetic foot ulcer patients. *Infect. Genet. Evol.* 92: 104824. https://doi.org/10.1016/j.meegid.2021.104824
24) Tribudi YA, Agustin AT, Setyaningtyas DE, Gusmalawati D (2022) Bioactive Compound Profile and Biological Modeling Reveals the Potential Role of Purified Methanolic Extract of Sweet
25) Flag (Acorus calamus L.) in Inhibiting the Dengue Virus (DENV) NS3 Protease-Helicase.
26) *Indones. J. Chem.* 22: 331–341. https://doi.org/10.22146/ijc.68317
27) Vestby LK, Grønseth T, Simm R, Nesse LL (2020) Bacterial Biofilm and its Role in the Pathogenesis of Disease. *Antibiotics* 9: 59. https://doi.org/10.3390/antibiotics9020059
28) Walicka M, Raczyńska M, Marcinkowska K, Lisicka I, Czaicki A, Wierzba W, Franek E (2021) Amputations of Lower Limb in Subjects with Diabetes Mellitus: Reasons and 30-Day Mortality. *J. Diabetes Res.* 2021: 1–8. https://doi.org/10.1155/2021/8866126